

1 Storage and Transport of Charge in
2 Redox Conductive Polymers
3 Probed with
4 Electron Spin Resonance Spectroscopy

5 **Ilia Romanovich Kulikov**

6 Im Fachbereich Physik der Freien Universität Berlin eingereichte
7 Dissertation zur Erlangung des Grades eines
8 Doktors der Naturwissenschaften

9 Berlin
10 August 2023

11
12
13
14

Erster Gutachter: Prof. Dr. Jan Behrends
Zweiter Gutachter: Prof. Dr. Kirill Bolotin
Tag der Disputation:

Contents

16	1 Introduction	5
17	2 Electrochemical Energy Storage in Redox Conductive Polymers	9
18	3 Operando EPR Spectroscopy of Energy Storage Materials	11
19	3.1 Electron Paramagnetic Resonance	11
20	3.1.1 Spin Hamiltonian	11
21	4 Pulsed Electron Paramagnetic Resonance Spectroscopy of Densely Packed Nitroxide Radicals	13
22	4.1 Coherent Spin Motion under Pulsed Microwave Field	13
23	4.2 Three-Dimensional Electron Gas with Inter-Spin Interactions	13
24	5 Longitudinally Detected Electron Paramagnetic Resonance in Systems with Short Relaxation	
25	Times	15
26	6 Electrically Detected Electron Paramagnetic Resonance on a Cathode of an Organic Radical	
27	Battery	17
28	6.1 Distribution of Current Density in On-Substrate Meander-Shaped Electrodes	17
29	7 The Deep-Trap Model of a TEMPO-Salen Electrode Film	21
30	8 Conclusions and Outlook	23

$\vec{e}_x, \vec{e}_y, \vec{e}_z, t$	Laboratory frame of reference
\vec{S}	Spin operator
\hat{S}_Z	Z component of the spin operator
$\mu_B = 9.2740100783(28) \times 10^{-24}$ J/T	Bohr magneton
$\mu_0 = 0.0000000000(00) \times 10^{-00}$ X/X	The permeability of free space
$\vec{B}_0 = B_0 \vec{e}_z$	Static magnetic field
ORB	organic radical battery
WE	working electrode (cathode)
CE	counter electrode (anode)
RE	reference electrode
SoC	state of charge
ESOC	EPR-detected SoC
CV	cyclic voltammogram
GCD	galvanostatic charge-discharge
TEMPO	2,2,6,6-tetramethylpiperidine-1-oxyl
pDiTBuS	poly-di-TEMPO-Butyl-Salen
PTMA	poly-TEMPO-methacrylate
EDFS	echo-detected field sweep
T_1	spin-lattice relaxation time
T_m	phase memory time
t_d	microwave detector dead time

Table 1: List of abbreviations

Chapter 1

Introduction

Life needs energy to continue its spread. Plants use photosynthesis to separate carbon from oxygen and to grow. Higher life forms as humans consume energy during the day and during the night, being dependent on the available energy source. While fossil fuels are still the major source of energy and while fire is used to convert the Joules that hold together hydrocarbon molecules into "horse power" of an engine and kilowatt-hours in the power socket, there are cleaner and more efficient ways to harvest energy. Photosynthesis had inspired the creation of solar panels that convert the sunlight into electricity, the atom had been tamed in the core of a nuclear reactor to power cities; we can extract the energy from sound, wind and waves and from the heat of the planet. Moreover, there are hopes and continuous attempts to achieve nuclear fusion - the creation of an artificial Sun by melting together atomic cores - the virtually inexhaustible and clean source of energy. The oil and gas are limited and unevenly distributed resources, and wind does not always blow, the Sun does not shine at night, the wild Nature is still unpredictable and the extracted energy has to be stored in order to level out its production and consumption.

With the rise of the technological era, over the last century, the energy has been delivered to our homes in form of electricity. The storage of electrical energy is the key ingredient of every power grid, every electrical device. Electric charges separated by a potential barrier can store energy in a device called a battery, or, precisely, a battery of electrochemical cells. It is also possible to store the energy in an electrostatic field between the plates of a capacitor, but due to the technological difficulties, electrochemical cells are commonly used nowadays. An electrochemical cell is an energy storage device that undergoes a chemical reaction to release electrical energy. A simple electrochemical cell consists of two spatially separated materials called electrodes, that have different work functions, or, chemically speaking, reduction-oxidation (redox) potentials. The electrodes are separated with a layer of ions that allow for the transfer of charge between the electrodes when they are connected to each other with a conductor that passes electric current through the consumer and therefore transfers the energy, that is, the battery is plugged into an electric circuit. While the battery delivers the electric current to the circuit, a chemical reaction is happening on its electrodes: the positively charged electrode, called cathode, is being reduced, obtaining electrons from the negatively charged anode, that accepts electrons and is being oxidized. The speed, reversibility, released by-products and physical conditions of this reaction are the key factors that define the performance of an electrochemical cell as an energy storage device. This reaction had been a great interest for the field of energy storage, particularly, electrochemistry, where numerous characterization techniques have been developed to optimize the architecture of batteries.

Stable, capacious and powerful batteries have become of great demand for today's energy driven society [47, 46, 33]. The advances in lithium ion technology for rechargeable batteries have enabled energy densities that make it possible to battery-power a wearable **Internet-of-things** device [23, 27], an airplane [18] or a house [4, 13]. Still, the application of lithium ion batteries is limited by irreversible

processes [22, 8, 50] that occur upon extreme operating conditions such as high power demand [49, 12] or over-discharge [26]. Such degradation processes limit the performance of a battery by lowering its safe operating power, resulting in lower power density and longer charging times. The challenge to overcome these limitations, together with low abundance of the rare earth metals [46] and the toxicity of the manufacturing process [35, 34] is motivating research and development of advanced battery technologies [3]. This requires understanding of charge transport and degradation pathways in energy storage materials as well as exploring novel materials such as materials based on organic precursors [25, 19].

Organic radical batteries (ORB) based on redox polymers containing stable radicals [30] have been shown to compete with or even outperform conventional Li based batteries in terms of power densities [41] with the additional benefit of being free from rare precursors, inheriting mechanical properties of plastics and electrical properties of semiconductors [7, 2, 10]. Advanced molecular design techniques allow for tuning of the electrochemical properties of the redox polymers [15], that brings in a rich variety of organic energy storage materials [45, 44, 16] and creates a large room for their optimization.

Redox conductive conjugated polymers containing TEMPO (2,2,6,6-tetramethylpiperidine-1-oxyl) redox groups, as pDiTBuS (poly-di-TEMPO-Butyl-Salen) shown in Figure 1.1, demonstrate particularly promising energy and power densities [43]. The pDiTBuS was designed as a cathode material: it is oxidized when the electrochemical cell containing this material is charged. A film of pDiTBuS comprises a high concentration of redox active stable nitroxyl radicals attached to a conjugated polymer backbone that interconnects them as a molecular wire. Such system can be viewed as a highly disordered molecular hole-transporting semiconductor (the poly-NiSalen backbone) that contains a large amount of hole traps (TEMPO groups) attached to it with butyl linkers. When the film is reduced (discharged), the TEMPO groups are in the radical state and act as unfilled traps. Upon oxidation (charging), the TEMPO fragments lose an unpaired electron and acquire a positive charge, so the traps are being filled with holes.

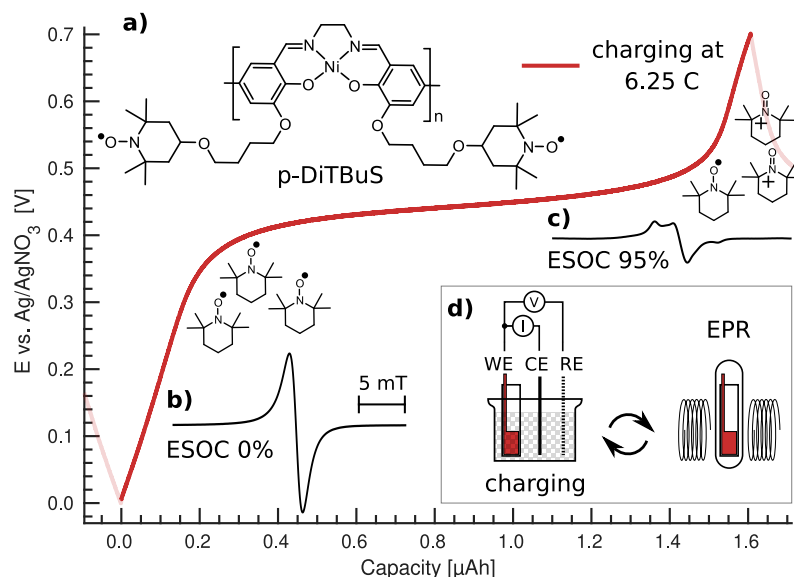


Figure 1.1: Galvanostatic charge-discharge curve for a pDiTBuS cathode film at 10 μA (6.25 C), chemical structure of pDiTBuS (a), normalized cwEPR spectral signatures for reduced (b) and oxidized (c) states. Scheme of the ex-situ EPR measurement on the pDiTBuS half cell (d).

The flexible molecular design together with questions regarding unresolved charge transport- and performance limiting mechanisms have inspired a variety of characterization techniques to be developed and applied to both energy storage materials and energy storage devices, operando and ex-situ. Together

95 with electrochemical characterization as the standard method for studying the properties of energy stor-
96 age materials[41, 48], operando optical microscopy [29], neutron imaging [26] and X-ray diffraction [36]
97 were applied to monitor irreversible structural deformations during extreme charging of Li cells.

98 UV and IR spectroscopy turned out to be particularly useful for studying organic energy-storage ma-
99 terials. For instance, it was possible to observe formation of positive polarons in the NiSalen backbone
100 of the pDiTBuS upon its oxidation [5]. Since the electrochemical processes happen within the bulk of
101 the energy storage material and involve changes in the spin states, imaging techniques based on mag-
102 netic resonance can be applied to obtain structural information on the battery electrodes on the molecular
103 level [32, 28, 24, 1]. NMR was used to study dendrite formation, electrolyte dynamics and intercalation of
104 Li ions[21, 11] in Li cells, including operando imaging [40].

105 Operando continuous-wave EPR (cwEPR) was applied to study redox kinetics of inorganic battery
106 cathodes [31], radical formation and spin densities in redox polymers [5] and in organic electrochemical
107 cells [14, 20].

108 Pulsed EPR (pEPR) provides an even more powerful toolbox for material studies with the electron spin
109 as a microscopic structural probe. In particular, pEPR provides access to the dipolar coupling between
110 neighboring electron spins and thus the possibility to determine distances between adjacent redox-active
111 centers using dipolar spectroscopy [37] as in spin-labelled proteins [17, 42]. In addition, the hyperfine
112 coupling between electron and nuclear spins in close vicinity can be measured by electron spin echo en-
113 velope modulation (ESEEM) and electron nuclear double resonance (ENDOR) techniques and can thus
114 elucidate the degree of delocalization for charge carriers in ORB materials in a similar way as in organic
115 semiconductors [6].

116 EDMR is allowing to manipulate the spin of an electron that tunnels through a disordered media such as
117 the amorphous silicon in a solar cell, through intertwined fragments of conjugated polymers in an organic
118 solar cell or an organic field-effect transistor.
119

120 **Chapter 2**

121 **Electrochemical Energy Storage in** 122 **Redox Conductive Polymers**

123 DiTS is a molecule that can efficiently store upto three electric charges. When polymerized, it can grow
124 into a film that performs well as a cathode in an electrochemical cell.

Chapter 3

Operando EPR Spectroscopy of Energy Storage Materials

3.1 Electron Paramagnetic Resonance

3.1.1 Spin Hamiltonian

The electron bears an internal angular momentum that is called spin. Spin combines with the charge of the electron to endow the electron with a magnetic moment. The magnetic moment of the electron is quantized: $\mu_e = \mu_B g S$ [9], where S is the spin quantum number, the eigenvalue of the spin operator \hat{S} , that equals $S = 1/2$ for an electron. When an electron is placed in a static magnetic field $\vec{B}_0 = B_0 \vec{e}_z$, its magnetic moment precesses about the field direction with the Larmor frequency $\omega_L = \gamma B_0$, where $\gamma = \frac{g_e \mu_B}{\hbar} = 28.025 \text{ GHz/T}$ is the gyromagnetic ratio of the electron and g_e is the electron g factor. The projection of the electron's magnetic moment on the direction of the magnetic field can take only discrete values between $-S = -1/2$ and $S = 1/2$, so that the eigenvalues of the z component of the spin operator are also discrete: $\hat{S}_Z |\uparrow\rangle = +\frac{\hbar}{2} |\uparrow\rangle$, $\hat{S}_Z |\downarrow\rangle = -\frac{\hbar}{2} |\downarrow\rangle$. The two eigenfunctions of \hat{S}_Z are called the spin-up state $|\uparrow\rangle$ and the spin-down state $|\downarrow\rangle$. The two corresponding eigenvalues $\pm \frac{\hbar}{2}$ define the energy difference between the states $|\uparrow\rangle$ and $|\downarrow\rangle$, that is known as the Zeeman splitting.

The energy of an unpaired electron placed in the external magnetic field \vec{B}_0 is the eigenvalue of the spin Zeeman Hamiltonian: $\hat{H}_{EZ} = \mu_B g \vec{B}_0 \cdot \vec{S}$. In the laboratory frame of reference $\vec{B}_0 \parallel \vec{e}_z$, $[\hat{H}_{EZ}, \hat{S}_z] = 0$, so \hat{H}_{EZ} and \hat{S}_z share the eigenfunctions $|\uparrow\rangle$ and $|\downarrow\rangle$. The Zeeman energies of the electron are $E_{EZ}^{\pm} = \pm \frac{\hbar}{2} \mu_B g B_0$.

A proton also bears an internal angular momentum $S = 1/2$ that results in a magnetic moment $\mu_p = \mu_e \frac{m_e}{m_p}$, that is $\frac{m_e}{m_p} \approx 1836$ times smaller than the electron's magnetic moment. A neutron bears no charge but still has an internal angular momentum $S = 1/2$. An atomic nucleus that consists of protons and neutrons can have a magnetic moment, depending on the mutual orientations of their spins and on the nuclear charge. A nitrogen nucleus has 7 protons and 7 neutrons that total in a nuclear spin $I = 1$ which, with the g factor for the nitrogen nucleus g_N , results in the nuclear magnetic moment of $\mu_N = \mu_B g_N \frac{m_e}{m_N} I$ that splits into three Zeeman energy levels corresponding to $I = -1, 0, +1$, analogously to the electron with $S = 1/2$. The nuclear Zeeman splitting is more than three orders of magnitude weaker than the electron Zeeman splitting because of the difference in the masses of the particles.

The magnetic moments of an electron and a magnetic nucleus, such as nitrogen, couple in the hyperfine interaction [38]: $H_{HF} = \vec{S} \mathbf{A} \vec{I} = H_F + H_{DD}$ with the hyperfine tensor \mathbf{A} . The isotropic part $H_F = a_{iso} \vec{S} \vec{I}$, or the Fermi contact interaction, scales with the probability density of the electron at the position of the nucleus $a_{iso} = \frac{2}{3} \frac{\mu_0}{\hbar} g_e \beta_e g_n \beta_n |\psi(0)|^2$. The anisotropic part $H_{DD} = \vec{S} \mathbf{T} \vec{I}$ with the dipolar coupling tensor \mathbf{T}

157 takes into account the anisotropic dipole-dipole coupling between the magnetic moments of the electron
 158 and the nucleus.

159 The nitrogen nucleus has a spin greater than 1/2 which alters the charge distribution within the nucleus
 160 which gives rise to a non-vanishing nuclear electrical quadrupole moment Q . The interaction between the
 161 asymmetrically distributed charge and the gradient of the electric field at the nucleus is given by the nuclear
 162 quadrupole Hamiltonian $H_{NQ} = \vec{I}\mathbf{P}\vec{I}$ with the nuclear quadrupole tensor \mathbf{P} that describes the coupling of
 163 the nuclear quadrupole moment to the electric field gradient.

164 In a system of closely placed electrons, such as in a film of densely packed nitroxide radicals, the elec-
 165 tron orbitals may overlap significantly and the radicals may exchange electrons. The energy required to
 166 exchange the electrons is called the Heisenberg exchange coupling $H_{exch} = \vec{S}_1\mathbf{J}\vec{S}_2$, that becomes consid-
 167 erably large at inter-spin distances below $r < 1.5$ nm or with a large spin delocalization [39]. The positive
 168 \mathbf{J} corresponds to a weak coupling between S_1 and S_2 which leads to an antiferromagnetic or antiparallel
 169 alignment of spins with a total $S = 0$, whereas the negative \mathbf{J} causes the strong inter-spin coupling which
 170 leads to a ferromagnetic alignment with $S = 1$.

171 The dipole-dipole interaction between the two neighboring electron spins contributes one more term to
 172 the spin Hamiltonian: $H_{dd} = \vec{S}_1\mathbf{D}\vec{S}_2$ that depends on the distance between the spins.

173 **Chapter 4**

174 **Pulsed Electron Paramagnetic** 175 **Resonance Spectroscopy of Densely** 176 **Packed Nitroxide Radicals**

177 **4.1 Coherent Spin Motion under Pulsed Microwave Field**

178 When a spin system is excited with a microwave pulse, its

179 **4.2 Three-Dimensional Electron Gas with Inter-Spin Interactions**

180 The observations of pulsed EPR spectra in densely packed nitroxide radicals have risen questions regard-
181 ing the physical model that would be able to describe these systems. So far no model for such system
182 could explain the results of the distorted EPR spectra and an attempt was made to introduce the inter-spin
183 interactions in the three-dimensional electron gas that appears to be the most accurate model of a polymer
184 cathode film.

185 **Chapter 5**

186 **Longitudinally Detected Electron** 187 **Paramagnetic Resonance in Systems** 188 **with Short Relaxation Times**

189 LOD lets us look behind the protection pulse.

Chapter 6

Electrically Detected Electron Paramagnetic Resonance on a Cathode of an Organic Radical Battery

With EDMR we observe the hopping charge as it travels to the charge bearing group through the electrode.

6.1 Distribution of Current Density in On-Substrate Meander-Shaped Electrodes

Meander-shaped electrodes shown in Figure 6.1 are used to study properties of thin conductive films. The distribution of electric potential and the current within a film of poor conductivity and a finite thickness be not obvious.

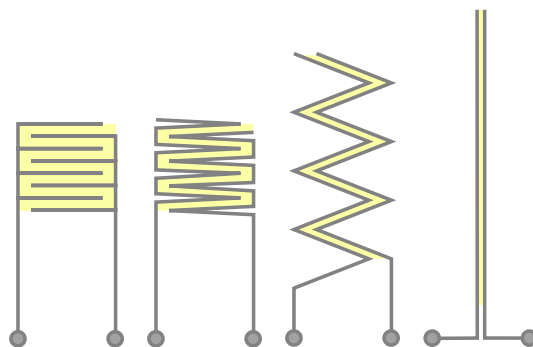


Figure 6.1: Transformation of the meander-shaped electrode grid into two linear electrodes

A numerical solution was found to the distribution of the current density \vec{j} within a film of a finite thickness, connected by two metal electrodes. Two cases were considered, a thick film and a thin film.

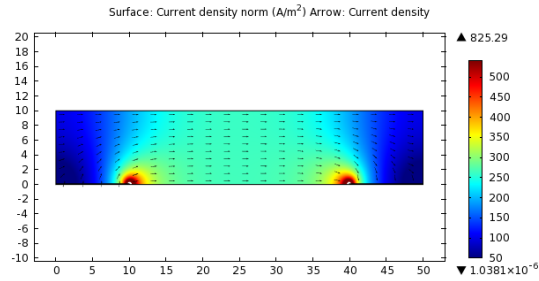


Figure 6.2: Distribution of electric current in a thick polymer film. The current is uniform in the middle of the film. **Let us see, whether we can apply the simple, bulk formula to this structure.**

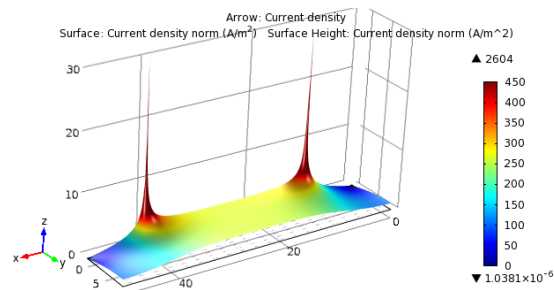


Figure 6.3: Thick film. The current is uniform in the middle of the film. It is better seen on this 3d plot. **Let us see, whether we can apply the simple, bulk formula to this structure. I think we do not gain a lot of error by saying that the current is uniform within the whole film.**

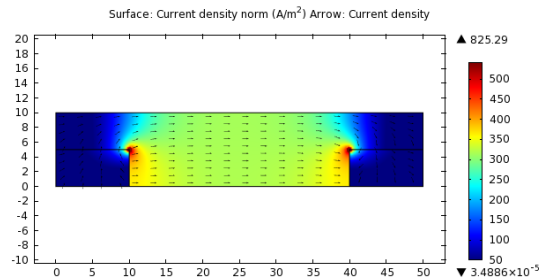


Figure 6.4: Distribution of electric current in an intermediate polymer film

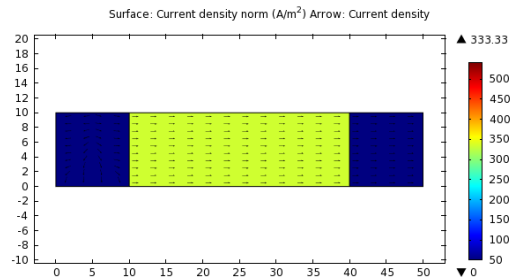


Figure 6.5: Distribution of electric current in a thin polymer film

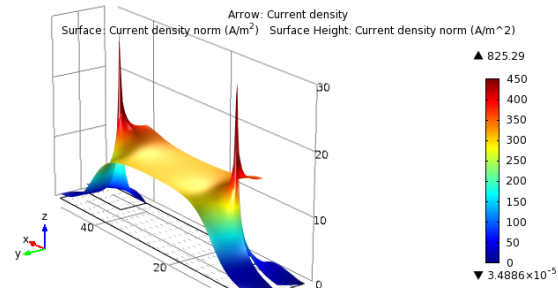


Figure 6.6: Very high values of the computed distribution of the current density in a film of intermediate thickness due to the sharp edges of the contacts.

203 **Chapter 7**

204 **The Deep-Trap Model of a** 205 **TEMPO-Salen Electrode Film**

206 A DiTBuS/DiTS film can be seen as a p-type, molecular semiconductor (the poly-Salen backbone) that
207 is heavily doped with low-energy traps for holes (TEMPO[•]).

208 **Chapter 8**

209 **Conclusions and Outlook**

210 What hasnt worked so far is the EDMR. It would be super cool to see the signal, but my devices don't
211 live that long. LOD also did not work up to now. Adjusting the pulse train rate to the eigenfrequency of
212 the ENDOR coils turned out to be an irresistible obstacle.

Bibliography

- [1] Robert Bittl and Stefan Weber. Transient radical pairs studied by time-resolved epr. *Biochimica et Biophysica Acta - Bioenergetics*, 1707:117–126, 2005.
- [2] Nerea Casado and David Mecerreyes. Chapter 1: Introduction to redox polymers: Classification, characterization methods and main applications, 2021.
- [3] Florian Degen and Marius Schütte. Life cycle assessment of the energy consumption and ghg emissions of state-of-the-art automotive battery cell production. *Journal of Cleaner Production*, 330:129798, 2022.
- [4] Boucar Diouf and Christophe Avis. The potential of li-ion batteries in ecowas solar home systems. *Journal of Energy Storage*, 22:295–301, 2019.
- [5] Evgenia Dmitrieva, Marco Rosenkranz, Julia S. Danilova, Evgenia A. Smirnova, Mikhail P. Karushev, Irina A. Chepurnaya, and Aleksander M. Timonov. Radical formation in polymeric nickel complexes with n2o2 schiff base ligands: An in situ esr and uv–vis–nir spectroelectrochemical study. *Electrochimica Acta*, 283:1742–1752, 2018.
- [6] M. Fehr, J. Behrends, S. Haas, B. Rech, K. Lips, and A. Schnegg. Electrical detection of electron-spin-echo envelope modulations in thin-film silicon solar cells. *Physical Review B - Condensed Matter and Materials Physics*, 84:1–5, 11 2011.
- [7] C Friebe and U S Schubert. High-power-density organic radical batteries. *Topics in Current Chemistry*, 375:1–35, 2017.
- [8] Yangyang Fu, Song Lu, Kaiyuan Li, Changchen Liu, Xudong Cheng, and Heping Zhang. An experimental study on burning behaviors of 18650 lithium ion batteries using a cone calorimeter. *Journal of Power Sources*, 273:216–222, 1 2015.
- [9] Walther Gerlach and Otto Stern. Der experimentelle nachweis der richtungsquantelung im magnetfeld. *Zeitschrift für Physik*, 9:348–352, 1922.
- [10] Nicolas Goujon, Nerea Casado, Nagaraj Patil, Rebeca Marcilla, and David Mecerreyes. Organic batteries based on just redox polymers: Abstract. *Progress in Polymer Science*, 122:101449, 2021.
- [11] Cristina Grosu, Chiara Panosetti, Steffen Merz, Peter Jakes, Stefan Seidlmayer, Sebastian Matera, Rüdiger a Eichel, Josef Granwehr, and Christoph Scheurer. Revisiting the storage capacity limit of graphite battery anodes : Spontaneous lithium overintercalation at ambient pressure. *PRX Energy*, 2:1–14, 2023.
- [12] Ting Guan, Shun Sun, Fengbin Yu, Yunzhi Gao, Peng Fan, Pengjian Zuo, Chunyu Du, and Geping Yin. The degradation of licoo2/graphite batteries at different rates. *Electrochimica Acta*, 279:204–212, 2018.
- [13] Takuma Hirasawa, Mika Yoshida, and Shin’ya Obara. Battery control for leveling the amount of electricity purchase in smart-energy houses. *International Journal of Energy Research*, 45:807–823, 2021.

- [14] Q Huang, E D Walter, L Cosimbescu, D Choi, and J P Lemmon. In situ electrochemical-electron spin resonance investigations of multi-electron redox reaction for organic radical cathodes. *Journal of Power Sources*, 306:812–816, 2016.
- [15] Tobias Janoschka, Christian Friebe, Martin D. Hager, Norbert Martin, and Ulrich S. Schubert. An approach toward replacing vanadium: A single organic molecule for the anode and cathode of an aqueous redox-flow battery. *ChemistryOpen*, 6:216–220, 2017.
- [16] Tobias Janoschka, Christian Friebe, Martin D. Hager, Norbert Martin, and Ulrich S. Schubert. An approach toward replacing vanadium: A single organic molecule for the anode and cathode of an aqueous redox-flow battery. *ChemistryOpen*, 6:216–220, 2017.
- [17] G Jeschke. Deer distance measurements on proteins. *Annual Review of Physical Chemistry, Vol 63*, 63:419–446, 2012.
- [18] Josef Kadlec, Radoslav Cipin, Dalibor Cervinka, Pavel Vorel, and Bohumil Klima. Li-ion accumulators for propulsion system of electric airplane vut 051 ray. *Journal of Solid State Electrochemistry*, 18:2307–2313, 2014.
- [19] Jihyeon Kim, Youngsu Kim, Jaekyun Yoo, Giyun Kwon, Youngmin Ko, and Kisuk Kang. Organic batteries for a greener rechargeable world. *Nature Reviews Materials*, 8:54–70, 2023.
- [20] Ilia Kulikov, Naitik A. Panjwani, Anatoliy A. Vereshchagin, Domenik Spallek, Daniil A. Lukianov, Elena V. Alekseeva, Oleg V. Levin, and Jan Behrends. Spins at work: probing charging and discharging of organic radical batteries by electron paramagnetic resonance spectroscopy. *Energy and Environmental Science*, 15:3275–3290, 2022.
- [21] T. Kushida and J. C. Murphy. Volume dependence of the knight shift in lithium. *Physical Review B*, 21:4247–4250, 1980.
- [22] Fredrik Larsson, Petra Andersson, Per Blomqvist, and Bengt Erik Mellander. Toxic fluoride gas emissions from lithium-ion battery fires. *Scientific Reports*, 7:1–13, 12 2017.
- [23] Yong Hee Lee, Joo Seong Kim, Jonghyeon Noh, Inhwa Lee, Hyeong Jun Kim, Sunghun Choi, Jeongmin Seo, Seokwoo Jeon, Taek Soo Kim, Jung Yong Lee, and Jang Wook Choi. Wearable textile battery rechargeable by solar energy. *Nano Letters*, 13:5753–5761, 2013.
- [24] Chao Li, Ming Shen, and Bingwen Hu. Solid-state nmr and epr methods for metal ion battery research. *Wuli Huaxue Xuebao/Acta Physico - Chimica Sinica*, 36:1–16, 2019.
- [25] Yong Lu and Jun Chen. Prospects of organic electrode materials for practical lithium batteries. *Nature Reviews Chemistry*, 4:127–142, 2020.
- [26] Tianyi Ma, Siyuan Wu, Fang Wang, Joseph Lacap, Chunjing Lin, Shiqiang Liu, Mohan Wei, Weijian Hao, Yunshi Wang, and Jae Wan Park. Degradation mechanism study and safety hazard analysis of overdischarge on commercialized lithium-ion batteries. *ACS Applied Materials and Interfaces*, 12:56086–56094, 2020.
- [27] Praveen Kumar Reddy Maddikunta, Gautam Srivastava, Thippa Reddy Gadekallu, Natarajan Deepa, and Prabadevi Boopathy. Predictive model for battery life in iot networks. *IET Intelligent Transport Systems*, 14:1388–1395, 2020.
- [28] Christoph Meier, Jan Behrends, Christian Teutloff, Oleksandr Astakhov, Alexander Schnegg, Klaus Lips, and Robert Bittl. Multi-frequency edmr applied to microcrystalline thin-film silicon solar cells. *Journal of Magnetic Resonance*, 234:1–9, 2013.
- [29] Alice J. Merryweather, Quentin Jacquet, Steffen P. Emge, Christoph Schnedermann, Akshay Rao, and Clare P. Grey. Operando monitoring of single-particle kinetic state-of-charge heterogeneities and cracking in high-rate li-ion anodes. *Nature Materials*, 21:1306–1313, 2022.

- [30] K Nakahara, S Iwasa, M Satoh, Y Morioka, J Iriyama, M Suguro, and E Hasegawa. Rechargeable batteries with organic radical cathodes. *Chem. Phys. Lett.*, 359:351–354, 2002.
- [31] Arvid Niemöller, Peter Jakes, Rüdiger A. Eichel, and Josef Granwehr. In operando epr investigation of redox mechanisms in LiCoO_2 . *Chemical Physics Letters*, 716:231–236, 2019.
- [32] Arvid Niemöller, Peter Jakes, Svitlana Eurich, Anja Paulus, Hans Kungl, Rüdiger A. Eichel, and Josef Granwehr. Monitoring local redox processes in $\text{LiNi}_{0.5}\text{Mn}_{1.5}\text{O}_4$ battery cathode material by in operando epr spectroscopy. *Journal of Chemical Physics*, 148:1–10, 2018.
- [33] Naoki Nitta, Feixiang Wu, Jung Tae Lee, and Gleb Yushin. Li-ion battery materials: Present and future. *Materials Today*, 18:252–264, 2015.
- [34] Jens F. Peters, Manuel Baumann, Benedikt Zimmermann, Jessica Braun, and Marcel Weil. The environmental impact of li-ion batteries and the role of key parameters – a review. *Renewable and Sustainable Energy Reviews*, 67:491–506, 2017.
- [35] Anna Pražanová, Vaclav Knap, and Daniel Ioan Stroe. Literature review, recycling of lithium-ion batteries from electric vehicles, part i: Recycling technology. *Energies*, 15:1–29, 2022.
- [36] Kevin J. Rhodes, Roberta Meisner, Melanie Kirkham, Nancy Dudney, and Claus Daniel. In situ xrd of thin film tin electrodes for lithium ion batteries. *Journal of The Electrochemical Society*, 159:A294–A299, 2012.
- [37] K. M. Salikhov, S. A. Dzuba, and A. M. Raitsimring. The theory of electron spin-echo signal decay resulting from dipole-dipole interactions between paramagnetic centers in solids. *Journal of Magnetic Resonance*, 42:255–276, 1981.
- [38] A Schweiger and G Jeschke. *Principles of Pulse Electron Paramagnetic Resonance*. Oxford University Press, 2001.
- [39] A Schweiger and G Jeschke. *Principles of Pulse Electron Paramagnetic Resonance*. Oxford University Press, 2001.
- [40] Yongchao Shi and Mingxue Tang. Nmr/epr investigation of rechargeable batteries. *Wuli Huaxue Xuebao/Acta Physico - Chimica Sinica*, 36:1–13, 2019.
- [41] Hiroyuki Takeo Nishide and Suga. Organic radical battery. *Journal of the Society of Mechanical Engineers*, 110:194–195, 2007.
- [42] Yu. V. Toropov, S. A. Dzuba, Yu. D. Tsvetkov, V Monaco, F Formaggio, M Crisma, C Toniolo, and J. Raap. Molecular dynamics and spatial distribution of toac spin-labelled peptaibols studied in glassy liquid by echo-detected epr spectroscopy. *Applied Magnetic Resonance*, 15:237–246, 1998.
- [43] Anatolii. A. Vereshchagin, Daniil A. Lukyanov, Ilia R. Kulikov, Naitik A. Panjwani, Elena A. Alekseeva, Jan Behrends, and Oleg V. Levin. The fast and the capacious: A $[\text{Ni}(\text{salen})]$ -tempo redox-conducting polymer for organic batteries. *Batteries & Supercaps*, 4:336–346, 2020.
- [44] Anatolii A. Vereshchagin, Arseniy Y. Kalnin, Alexey I. Volkov, Daniil A. Lukyanov, and Oleg V. Levin. Key features of tempo-containing polymers for energy storage and catalytic systems. *Energies*, 15:1–50, 2022.
- [45] Yuan Xie, Kai Zhang, Yusuke Yamauchi, Kenichi Oyaizu, and Zhongfan Jia. Nitroxide radical polymers for emerging plastic energy storage and organic electronics: Fundamentals, materials, and applications. *Materials Horizons*, 8:803–829, 2021.
- [46] Chengjian Xu, Qiang Dai, Linda Gaines, Mingming Hu, Arnold Tukker, and Bernhard Steubing. Future material demand for automotive lithium-based batteries. *Communications Materials*, 1:1–10, 2020.

- [47] Hyun Deog Yoo, Elena Markevich, Gregory Salitra, Daniel Sharon, and Doron Aurbach. On the challenge of developing advanced technologies for electrochemical energy storage and conversion. *Materials Today*, 17:110–121, 2014.
- [48] Clara Zens, Christian Friebe, Ulrich S. Schubert, Martin Richter, and Stephan Kupfer. Tailored charge transfer kinetics in precursors for organic radical batteries – a joint synthetic-theoretical approach. *ChemSusChem*, e202201679:1–14, 2022.
- [49] Guangxu Zhang, Xuezhe Wei, Siqi Chen, Guangshuai Han, Jiangong Zhu, and Haifeng Dai. Investigation the degradation mechanisms of lithium-ion batteries under low-temperature high-rate cycling. *ACS Applied Energy Materials*, 5:6462–6471, 2022.
- [50] Qingsong Zhang, Tiantian Liu, and Qiong Wang. Experimental study on the influence of different heating methods on thermal runaway of lithium-ion battery. *Journal of Energy Storage*, 42:1–9, 10 2021.